Landslide Stability: Role of Rainfall-Induced, Laterally Propagating, Pore-Pressure Waves

GEORGE R. PRIEST[1]

Oregon Department of Geology and Mineral Industries, P.O. Box 1033, Newport, OR 97365

WILLIAM H. SCHULZ

WILLIAM L. ELLIS

U.S. Geological Survey, Denver Federal Center Box 25046, MS 966, Denver, CO 80225-0046

JONATHAN A. ALLAN

Oregon Department of Geology and Mineral Industries, P.O. Box 1033, Newport, OR 97365

ALAN R. NIEM

WENDY A. NIEM

Pacific Geology Northwest LLC, 6325 B Avenue, Otter Rock, OR 97369

Key Terms: ***Translational Landslide, Hydrogeology, Rainfall, Pore Pressure, Johnson Creek, Oregon***

ABSTRACT

The Johnson Creek Landslide is a translational slide in seaward-dipping Miocene siltstone and sandstone (Astoria Formation) and an overlying Quaternary marine terrace deposit. The basal slide plane slopes sub-parallel to the dip of the Miocene rocks, except beneath the back-tilted toe block, where it slopes inland. Rainfall events raise pore-water pressure in the basal shear zone in the form of pulses of water pressure traveling laterally from the headwall graben down the axis of the slide at rates of 1–6 m/hr. Infiltration of meteoric water and vertical pressure transmission through the unsaturated zone has been measured at ∼50 mm/hr. Infiltration and vertical pressure transmission were too slow to directly raise head at the basal shear zone prior to landslide movement. Only at the headwall graben was the saturated zone shallow enough for rainfall events to trigger lateral pulses of water pressure through the saturated zone. When pressure levels in the basal shear zone exceeded thresholds defined in this paper, the slide began slow, creeping movement as an intact block. As pressures exceeded thresholds for movement in more of the slide mass, movement accelerated, and differential displacement between internal slide blocks became more pronounced. Rainfall-induced pore-pressure waves are probably a common landslide trigger wherever effective hydraulic conductivity is high and the saturated zone is located near the surface in some part of a slide. An ancillary finding is apparently greater accuracy of grouted piezometers relative to those in sand packs for measurement of pore pressures at the installed depth.

INTRODUCTION

There is large body of theoretical and empirical data on the role of rainfall-induced pore-pressure increases in triggering debris flows and earth flows (e.g., see summary by Iverson, 2000) but little on translational bedrock slides. Empirical demonstration of theoretical work has generally focused on downward infiltration into very shallow (∼1–3 m deep) soils and subsequent rapid increases in pore pressures triggering landslide movement and debris flows soon after the onset of intense rainfall or snowmelt (e.g., Torres et al., 1998; Montgomery et al., 2002), or, in the case of deeper landslides, delayed increases in pore pressure from downward infiltration that triggers movement weeks to months after a rainfall event (e.g., Iverson and Major, 1987; Calabro et al., 2010). Pore-pressure increases and resultant movement of some

[1]Corresponding author email: george.priest@dogami.state.or.us.

deep landslides have been observed very soon after rainfall or snowmelt (e.g., Corominas et al., 2005; Schulz et al., 2009a), and this is usually attributed to very shallow groundwater depths or infiltration through fractures. Baum and Reid (1995) found that a clay-rich slide moved from vertical transmission of rainfall-induced pore pressures, but only after the groundwater table reached nearly to the surface. The Johnson Creek Landslide is a deep (~7–30 m) translational slide in fractured Tertiary sedimentary rocks that moves in response to pore-pressure increases within hours to a few days after intense winter rainfall events, although the groundwater table is quite deep (~5–20 m) throughout most of the slide. We analyzed this deep landslide to evaluate the mechanisms for this rapid reactivation. We performed detailed surface and subsurface characterization of geologic conditions of the landslide, its kinematics, and its hydrology. Much of our work entailed continuous monitoring of its movement and hydrology from November 23, 2002, to April 1, 2007. The central question that we answer in this paper is: Can vertical infiltration or vertical pore-pressure transmission trigger movement in this type of slide, or is lateral pore-pressure transmission the principal trigger? Earlier papers (Landslide Technology, 2004; Priest et al., 2008) describe stability evaluations of the landslide performed using limit-equilibrium analyses.

Study Area

The Johnson Creek Landslide (Figure 1) is one of several similar translational slides on the coastal bluffs of Lincoln County, Oregon, that cut through seaward-dipping Tertiary sedimentary rocks (Priest and Allan, 2004). When these bluffs form sea cliffs 20–60 m high, translational slides are common, with single block failures on the order of ~100 m in width (Priest and Allan, 2004). The bluff at Johnson Creek has all of these characteristics: It is ~30 m high, is composed of seaward-dipping Miocene siltstone and sandstone of the Astoria Formation, and is affected by a large translational landslide ~200 m wide (Figure 1). Like many of the sedimentary rock bluffs on the Pacific coast, a flight of Pleistocene marine terraces creates a step-like landscape with a veneer of Pleistocene beach and dune sand. The landslide cuts through the second youngest terrace in this sequence.

METHODS

Data Acquisition

The slide was examined on the surface by detailed topographic and geologic mapping. Movement of the slide between October 2002 and April 2003 (the largest wet season movement in 5 years of observation) was determined at the ground surface by surveying, using a total station survey, pins along a line-of-sight parallel to the Oregon Coast Highway (precision of ±0.5 cm) and steel stakes (precision of ±11–15 cm horizontal, ±6 cm vertical) placed in three lines from the head to toe of the slide (for detailed descriptions and data, see Priest et al., 2008). Hand measurements with a ruler of the heads of marker nails installed on both sides of well-defined scarps (precision of ±0.1 cm) provided additional displacement data for movement between March 12 and April 11, 2003. Movement in the subsurface was monitored episodically between October 2002 and January 2003 using three borehole inclinometers (Figure 1). We examined the slide in the subsurface using a 1.5-m-deep test pit at the toe and five boreholes within the landslide (Figure 1). Several parameters were monitored continuously (15 minute to 1 hour intervals) using solar- and battery-powered data loggers during various periods between October 2002 and April 2007: Landslide movement was monitored by three inclinometers (LT-1, LT-2, and LT-3; Figure 1) that were converted to extensometers passing through inclinometer casings and anchored beneath the slide; hydrological conditions were monitored using vibrating-wire piezometers and soil moisture probes; and rainfall was monitored by a rain gauge at the head of the slide (Figure 1). After inclinometer measurements in December 2002 established the location of the basal shear zone, vibrating-wire piezometers (LT-1p, LT-2p, and LT-3p; Figure 1) were installed next to the inclinometers, each in ~3 m of silica sand that reaches or penetrates the base of the basal shear zone (Table 1). Each sand pack was isolated hydrologically by bentonite above and, in the case of the middle (LT-2p) borehole, below the sand pack as well. The latter hole also had a piezometer installed below the slide, but the connection was sheared off by movement before meaningful data could be retrieved. In the last 4 months of the project, vertical arrays of vibrating-wire piezometers were installed at the western (LT-1) and middle (LT-2) observation sites, each in a bentonite-grout mixture (approximately 0.1:0.4:1 of bentonite:cement:water by weight). This mixture has an approximate hydraulic conductivity of 10^{-8} m/s (Mikkelsen and Green, 2003; Contreras et al., 2008). As demonstrated theoretically, in the laboratory, and in field settings (Vaughan, 1969; McKenna, 1995; and Contreras et al., 2008), grouting of piezometers has no effect on measurement accuracy if the conductivity of the grout is at most 1,000 times greater than conductivity of the geologic formation. The grout we used has lower

Figure 1. Site map of the Johnson Creek Landslide showing the 2002–2006 drill sites, soil moisture probes, and the rain gauge. Borehole labels ending in "a" or "p" have piezometers; boreholes LT-1, LT-2, and LT-3 have inclinometer casing. WC-1S, WC-3S, and WC-3D are soil moisture probes.

conductivity than the Johnson Creek Landslide because the lower bound for conductivity of unfractured siltstone bedrock is on the order of 10^{-7} m/s (e.g., Fetter, 1994). Bentonite-grout backfill was used because (1) it permits accurate readings of pore pressures in vertical arrays, (2) it results in shorter lag time than sand backfill, and (3) it provides a high-air-entry media, permitting measurement of negative (suction) pressures (e.g., McKenna, 1995; Contreras et al., 2008). We were interested in observing changes in pore pressures above the groundwater table as well as below. The history of geotechnical installations is summarized in Table 2. Depths of boreholes, soil moisture probes, and piezometers are summarized in Table 1. Additional details of borehole construction and instrumentation are given in Schulz and Ellis (2007) and Priest et al. (2008).

RESULTS

Slide Structure

All available evidence indicates that the Johnson Creek Landslide is a 200-m-long translational slide with a back-rotated passive toe wedge (Figure 2). The basal slide plane, as defined by the three inclinome-

Table 1. *Depths and elevations of the ground surface, piezometers, and soil moisture probes relative to the base of the basal shear zone ("slide plane" in the table).*

Hole	Site	Borehole Elevation (m)	Total Depth (m)	Depth to Probe Tip (m)	Probe Elevation (m)	Slide Plane Depth (m)	Slide Plane Elevation (m)	Sand-Pack Depth Interval (m)
LT-1p piezo. @ 24.80 m	West	25.179	26.8	24.80	0.38	26.2	−1.1	23.8–26.8
LT-1 inclinometer	West	25.048	33.8			26.5	−1.5	–
LT-2p piezo. @ 16.70 m	Middle	24.698	25.0	16.70	8.00	18.4	6.3	15.2–18.2
LT-2p piezo. @ 24.70 m	Middle	24.698	25.0	24.70	0.00	18.4	6.3	21.8–25.0
LT-2 inclinometer	Middle	25.028	34.7			18.6	6.4	–
LT-3p piezo. @ 5.5 m	East	24.472	7.0	5.50	18.97	5.8	18.7	3.9–7.0
LT-3 inclinometer	East	24.746	28.7			7.0	17.7	–
LT-1A piezo. @ 3.35 m	West	25.201	26.5	3.35	21.85	25.9	−0.7	Grouted
LT-1A piezo. @ 9.14 m	West	25.201	26.5	9.14	16.06	25.9	−0.7	Grouted
LT-1A piezo. @ 15.24 m	West	25.201	26.5	15.24	9.96	25.9	−0.7	Grouted
LT-1A piezo. @ 21.34 m	West	25.201	26.5	21.34	3.86	25.9	−0.7	Grouted
LT-1A piezo. @ 24.08 m	West	25.201	26.5	24.08	1.12	25.9	−0.7	Grouted
LT-1A piezo. @ 26.21 m	West	25.201	26.5	26.21	−1.01	25.9	−0.7	Grouted
LT-2A piezo. @ 3.05 m	Middle	24.792	19.4	3.05	21.74	18.8	6.0	Grouted
LT-2A piezo. @ 6.10 m	Middle	24.792	19.4	6.10	18.69	18.8	6.0	Grouted
LT-2A piezo. @ 10.67 m	Middle	24.792	19.4	10.67	14.12	18.8	6.0	Grouted
LT-2A piezo. @ 13.72 m	Middle	24.792	19.4	13.72	11.07	18.8	6.0	Grouted
LT-2A piezo. @ 16.76 m	Middle	24.792	19.4	16.76	8.03	18.8	6.0	Grouted
LT-2A piezo. @ 19.29 m	Middle	24.792	19.4	19.29	5.50	18.8	6.0	Grouted
WC-1S soil moisture probe @ 1.5 m	West	25.048	1.50	1.50	23.55	26.5	−1.5	–
WC-3S soil moisture probe @ 1.6 m	East	24.396	1.60	1.60	22.80	7.0	17.4	–
WC-3D soil moisture probe @ 3.1 m	East	24.396	3.10	3.10	21.30	7.0	17.4	–

Piezo. = piezometer; @ = at depth of; all elevations are relative to NAVD88.

Table 2. *Summary of work on the Johnson Creek Landslide that is utilized in this paper.*

Date	Project Work	Reference
October 2002–January 2003	October 2002 topographic survey + survey of marker pins and rain gauge installation; October–December 2002 drilling of paired inclinometer-piezometer boreholes at three sites in a line from the headwall to the lower part of the slide. Piezometer and rainfall data collected hourly. Slide movements from December 2002 to January 2003 prevented inclinometer logging (precision = ±0.25 mm), so all inclinometers were converted to extensometers (precision = ±1 cm) by January 3, 2003.	Landslide Technology (2004); Priest et al. (2006, 2008)
March–May 2003	Surface movements determined by April 17, 2003, survey of marker pins (precision = ±11–15 cm horizontal, ±6 cm vertical), line-of-sight surveys down coast highway (precision = ±0.5 cm), and by hand measurements between marker nails on fresh slide scarps (precision = ±0.1 cm); test pit excavated at slide toe.	Priest et al. (2006, 2008)
2004	Limit equilibrium stability modeling for winter 2002–2003 season monitoring data.	Landslide Technology (2004); Priest et al. (2006, 2008)
2004	November 20, 2004, USGS installs data loggers to automatically record movement at the three extensometers (precision = ±0.5 mm; accuracy = ±4 mm) simultaneously with piezometer and rainfall data.	Ellis et al. (2007a, 2007b), Schulz and Ellis (2007)
December 2006	Vertical arrays of grouted piezometers installed at the middle and west drill sites; soil moisture probes installed at the eastern and lower western sites. USGS website posted showing real-time monitoring data: http://landslides.usgs.gov/monitoring/johnson_creek/	Priest et al. (2008, 2009), Schulz (2007), Schulz et al. (2009b)
2007	USGS open-file report on monitoring data for last 2.5 years of collection: http://pubs.usgs.gov/of/2007/1127/	Schulz and Ellis (2007)
2008	DOGAMI Special Paper on 5 years of monitoring data plus modeling.	Priest et al. (2008)

USGS = US Geological Survey; DOGAMI = Oregon Department of Geology and Mineral Industries.

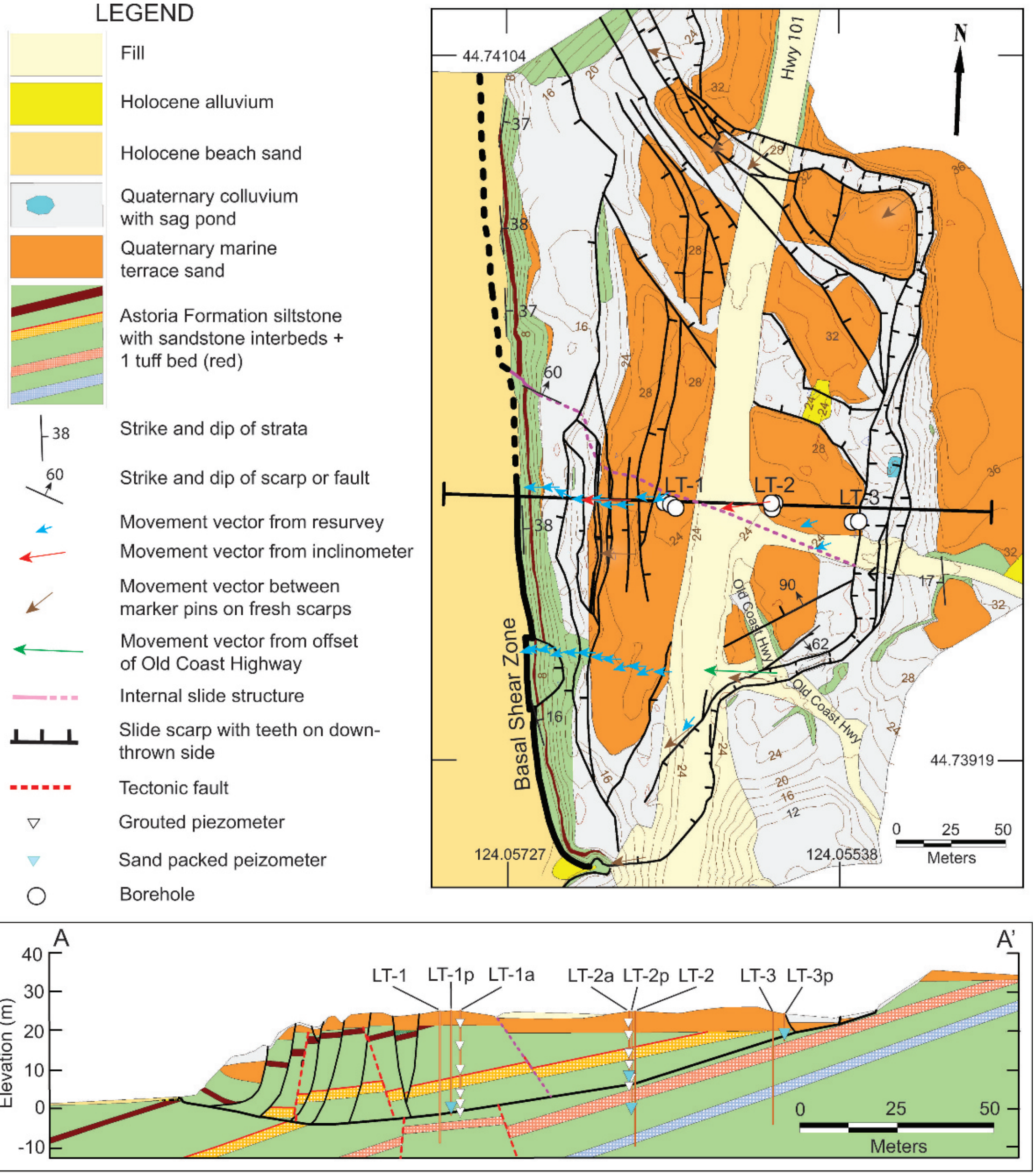

Figure 2. Geologic map and cross section. Topographic contours are at intervals of 2 m relative to NAVD88; blue arrows are direction of movement from surveys of steel markers between October 24, 2002, and April 17, 2003; brown arrows are direction of movement between March 12 and April 11, 2003, from marker nails on fresh slide scarps. Strike and dip of tectonic faults (red dashed lines in cross section) are inferred and cannot be located more accurately than the spacing of the boreholes, so they are not depicted on the geologic map. Vertical scale equals horizontal scale in cross section.

ters, is curving but sub-parallel to the seaward dip of the Tertiary Astoria Formation (~17 degrees west). The slide plane surfaces at the beach, where a test pit revealed it dipping landward and over-riding Holocene sand and colluvium. This reversal at the slide toe of the westward dip of the slide plane and westward dip of the Astoria Formation (15–45 degrees east at the toe) is evidence for back-tilting of the toe block by up to 62 degrees. The 6–15 m headscarp lies above a headwall graben, 7–23 m wide, behind the much wider translational slide block (Figure 1). The Pleistocene marine terrace is vertically offset 21 m from the headscarp to the slide toe. In the central part of the slide, the contact of the Pleistocene marine terrace sand with the underlying Astoria Formation is 2 m lower in boreholes LT-2 and LT-3 than in LT-1 to the west (Figure 2). Lacking evidence of a Quaternary fault in the area, an internal slide structure is inferred between boreholes LT-1 and LT-2 with apparent dip of 58 degrees east. This apparent dip is reasonably well constrained by measured offsets of the sub-horizontal Pleistocene terrace and west-dipping marker beds identified in cores of the Astoria Formation. A similar structure occurs in the toe block (Figure 2).

There are no direct measurements of hydraulic conductivity of the slide mass, but the highly fractured rock should provide ready pathways for lateral and vertical flow of groundwater. The rock matrix at the three drill sites consists of moderately to highly fractured sandstone, siltstone, and tuffaceous mudstone of the Astoria Formation overlain by 5–7 m of Pleistocene marine terrace sand. While the terrace sand is very well sorted and probably highly permeable, the Astoria Formation has 24–4 percent clay and 17–93 percent silt, which effectively limit the permeability of the rock matrix (see Appendix A of Priest et al., 2008). Permeability values for Astoria Formation with similar percentages of silt and clay are ~3–31 millidarcies (Snavely et al., 1964). Gouge material at the basal slide plane is very soft, slightly clayey to clayey, sandy silt. Brecciated siltstone and sandstone were commonly encountered in the slide debris, especially at the basal shear zone, but were not encountered in the rock below the slide. In exposures at the toe of the slide, spacing of tectonic joints in Astoria Formation below the slide plane tends to be irregular, with some areas nearly devoid of joints over distances of a few meters next to areas with sets of joints spaced at a few tenths of a meter. On the face of the sea cliff, extensional high-angle fractures parallel to the cliff face have normal listric slip of a few to several meters. An exposure at the sea cliff on the north side of Johnson Creek has fracture systems spaced at an average of 12 cm, with many only a few centimeters apart. Fractures in the slide are generally stained by apparent iron oxidation, occurring in three major sets, N47°E, 32–42°W, and N7–17°E with sub-vertical dip. No preferred orientation could be documented, except a general observation that the most closely spaced fractures tend to occur at and are parallel to major internal block boundaries. This fracture pattern was apparent in fresh exposures of fractured Pleistocene marine terrace sand blocks near the head of the slide.

The fractured Tertiary rock and overlying fractured marine terrace sand are covered by a thin (<1.5 m) veneer of sandy soil in most areas of the slide, except at the head graben, where colluvial sand and rock fragments fill former fissures to at least a few meters depth. There are no direct measurements of the hydraulic conductivity of this soil and colluvium, but the high sand content probably promotes water infiltration. This hypothesis is supported by the observation that large rainfall events seldom result in standing water, except at the head graben, where the groundwater table is near or at the surface. However, sparse wetland plants do occur on the marine terrace sand in a few small (10 m) areas, indicating locally perched groundwater.

Slide Movement from Surface Observations: 2002–2003

Surface monitoring revealed slide movement downslope away from the slide perimeter, with fastest movement in the southwest quadrant. Survey points were established on the ground surface at three east-west sections across the slide; two of the sections had movement larger than measurement error (Figure 3). Readings were taken on October 24, 2002, and April 17, 2003, bracketing the period of largest known continuous slide movement. The direction of this slide movement was generally parallel to the slide axis (Figure 2). Based on readings taken upslope of the headwall graben in stable ground, the survey repeatability error is large, about 11 cm to 15 cm horizontal and 1 to 130 cm vertical. The one point with 130 cm vertical error is not typical and was probably the result of disturbance of the steel stake or calculation/transcription error; vertical error was generally ±6 cm. At the drilling transect (Figure 1), horizontal surface displacement was 22 to 33 cm to the west to southwest and 4–9 cm vertical (Figure 3). Largest movement was in the southern survey line, where the slide moved 21–131 cm horizontal and 6–70 cm vertical (Figure 3). Line-of-sight survey readings taken in January and February 2003 along Highway 101 also show that the southern part of the slide moved more than the north part (Priest et al., 2008). The survey data are consistent with December 2002 measurements of vertical displacement of Highway 101 of only ~1–2 cm vertical on the northern margin but 18 cm vertical on the southern margin (for data, see Priest et al., 2008).

Data from marker nails are consistent with *en mass* movement of the entire slide during a small movement event in March 2003 (for data, see Priest et al., 2008). On March 12, 2003, marker nails were placed across fresh scarps created from the large January 2003 slide movement and then measured on March 24 and April 11, 2003. A slide movement episode measured at ~2 ± 0.1 cm at the three extensometers during March 21–28 displaced all of the nails around the slide perimeter by ~2 cm. Direction of motion determined from the nails was westward at the headwall graben, right lateral at the north margin, and left lateral at the southern margin, consistent with

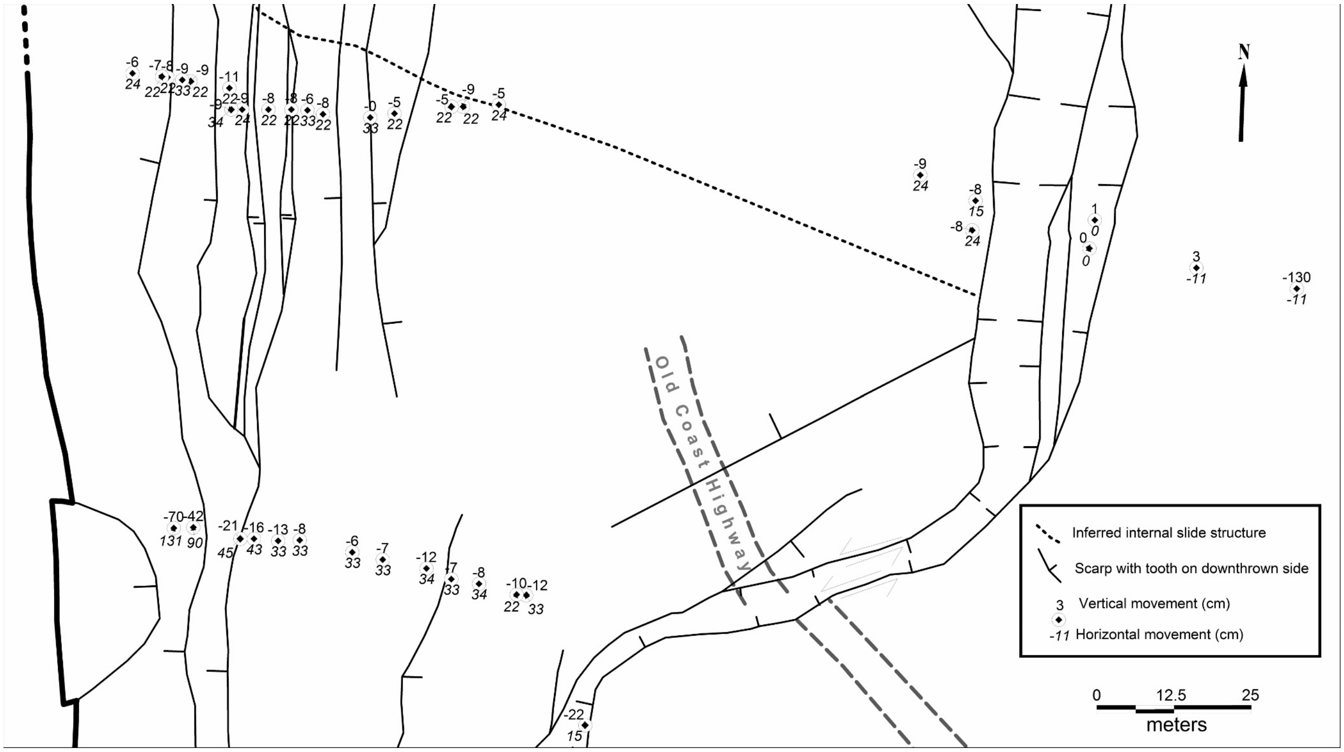

Figure 3. Vertical and horizontal displacement of steel survey markers from October 24, 2002, to April 17, 2003. Vertical movement down is negative; horizontal movement west toward the slide toe is positive. Movements east of the headwall of the slide are presumed to be errors, since this area has no other evidence of ground movement.

survey and inclinometer data (see movement vectors, Figure 2A). Nails placed across an older, sharply defined bedrock scarp in the interior of the slide showed no differential movement (east-northeast–trending scarp with a 90 degree dip in southeast part of slide; Figure 2).

Slide Movement from Subsurface Observations: 2002–2007

Shear movement was detected in December 2002 inclinometer measurements at depths of 26.5, 18.6, and 7.0 m below ground surface from west to east in LT-1, LT-2, and LT-3, respectively (Table 1). Landslide Technology (2004) places the slide plane near the bottom of the shear zone deflection in inclinometer data (Table 1; for inclinometer plots, see Landslide Technology [2004] or Priest et al. [2008]). All shear displacement of the inclinometer casings occurred within a 1.2-m-thick zone, indicating that the basal shear zone at these locations is less than 1.2 m thick (Schulz and Ellis, 2007). About 64 percent and 83 percent of the shear displacement of the inclinometer casing at boreholes LT-1 and LT-2, respectively, occurred within a 0.6-m-thick zone, strongly suggesting that the basal shear zone at these locations is less than 0.6 m thick (Schulz and Ellis, 2007). Core logging (Landslide Technology, 2004) was unable to conclusively identify the basal shear zone in any borings, although fracturing decreased at a depth of 26.2 m in LT-1, slickensides were observed at a depth of 18.1 m in LT-2, and core recovery was 51–93 percent for these two borings where sampling crossed the location of the basal shear zone, as indicated by inclinometer monitoring. Inclinometers LT-1, LT-2, and LT-3 measured shear zone movement vectors in the directions 273, 258, and 247 degrees azimuth, respectively (red arrows in Figure 2). These directions were consistent with the survey and marker pin data (blue arrows in Figure 2).

Total slide displacement measured at the boreholes over the 5 years was ~37 cm at the western site (LT-1), ~45 cm at the middle site (LT-2), and ~25 cm at the eastern site near the headwall graben (LT-3) (Figure 4A and Table 3). Inclinometer readings began on December 11, 2002. Shear movement was first detected in the casings on December 16, 2002. Displacements of 2.3 to 3.2 cm at the slide plane caused enough distortion of inclinometer casing to prevent passage of the logging device (Figure 4A). Each inclinometer was converted to an extensometer when this happened. Excessive slide movement that precluded the continued use of inclinometers progressed from the toe (west) to the head of the slide

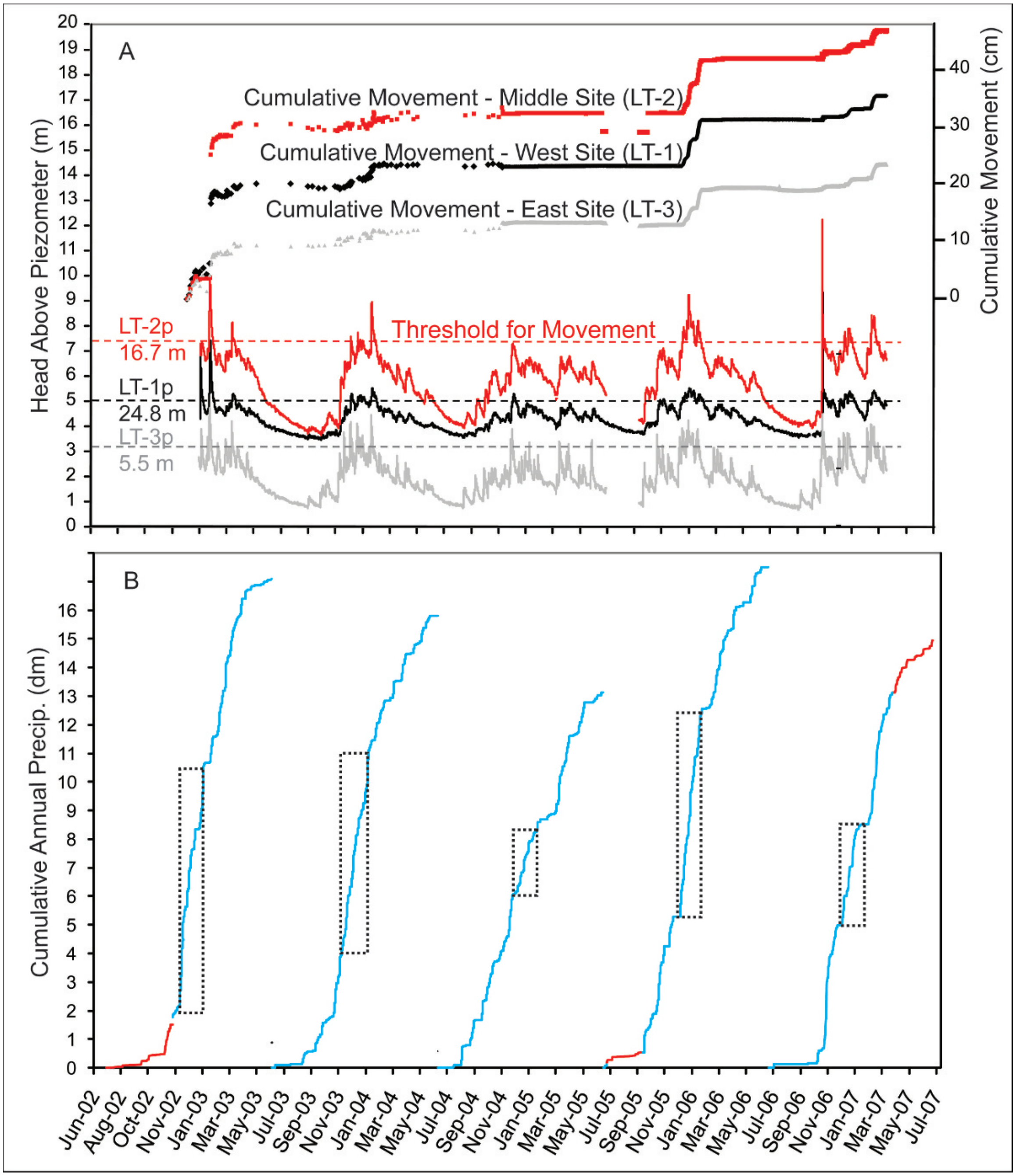

Figure 4. (A) Piezometer response and cumulative movement. Piezometer data are from sand-packed piezometers in the basal shear zone at the depths listed below the piezometer numbers, LT-1p, LT-2p, and LT-3p. Threshold = approximate pressure head where slide movement generally occurred at each piezometer. (B) Cumulative precipitation per water year (July 1 to June 30). Dotted boxes illustrate cumulative precipitation from December 1 to February 1 of each year. This interval was associated with the largest rainfall event that preceded the largest slide movement on February 1, 2003. Blue lines are data from the local rain gauge; red lines are data from the Hatfield Marine Science Center (HMSC), 12 km south of the study area.

(east): December 23, 2002, for LT-1, December 26 for LT-2, and January 3, 2003, for LT-3. The middle drill site (LT-2) generally moved further than the other two sites, except during the initial movements in December 2002, when the west site (LT-1) moved ~1 cm further than the middle site (Table 3). The east site (LT-3) generally lagged behind the others, except for an anomalous apparent movement on November 19, 2004, which was probably related to the instrumentation upgrade that occurred on that day, and a

Table 3. *Displacement for each movement event episode. Differences of 1–2 cm in total inferred movement between this table and Figure 4A are caused by accumulated rounding errors in extensometer data collected after inclinometer readings in December 2002 but before automated data collection began on November 20, 2005; those data have measurement errors of ±1 cm.*

Episode	West Site (LT-1) (cm)	Middle Site (LT-2) (cm)	East Site (LT-3) (cm)
Dec. 13–31, 2002	5	4	3.2
Jan. 31–Feb. 3, 2003	14	24	5
Mar. 21–28, 2003	2	2	2
Nov. 15, 2003–Mar. 4, 2004	4	2	3
Nov. 11–19, 2004	0	0	2
Dec. 27, 2005–Jan. 4, 2006	1.4	1.4	1.0
Jan. 6–24, 2006	3.3	3.5	1.8
Jan. 27–Feb. 10, 2006	3.4	4.0	3.2
Nov. 6–15, 2006	0.6	1.1	0.6
Dec. 24–28, 2006	0.3	0.2	0.3
Jan. 2–11–2007	1.1	1.0	0.9
Feb. 15–16, 2007	0.0	0.0	0.2
Feb. 25–Mar. 9, 2007	2.2	2.2	2.2
Mar. 12–15, 2007	0.0	0.0	0.1
TOTAL	**37**	**45**	**25**

February 15–16, 2007, movement of 0.2 cm (Figure 4 and Table 3). The 24 cm displacement at LT-2 between January 31 and February 3, 2003, created 10 cm of contraction in the lower part of the slide (between LT-1 and LT-2) and 19 cm of extension in the upper part (between LT-3 and LT-2) (Table 3).

Rainfall

Most rainfall occurred between the middle of September and May in each of the five monitored winters; the most intense precipitation was between November and February each year (Figure 4B). Total rainfall for each water year was highest in 2005–2006, followed by 2002–2003, 2003–2004, 2006–2007, and 2004–2005. December 1–February 1 rainfall was highest in 2002–2003, followed by 2005–2006, 2003–2004, 2006–2007, and 2004–2005(dotted rectangles in Figure 4B); slide movement followed the same pattern (Figure 4A).

Groundwater

Soil Moisture Data

At the west site (borehole LT-1), the probes were installed in Pleistocene marine terrace sand with negligible soil veneer. At the east site (borehole LT-3), probes were in 1.3 m of loose brown, clayey, silty fine sand with woody organics (fill) and underlying marine terrace sand (Landslide Technology, 2004). The probe at 1.6 m depth at the east site (probe WC-3s) had less pronounced and slower response to wetting events than the one at 1.5 m depth at the west site (probe WC-1s; Figure 5).The soil moisture probe at 3.1 m depth at the east site responded to major rainfall events before the probe at 1.6 m depth and contemporaneously with total piezometric head reaching 1 m above the probe elevation (Figures 5 and 6); hence, the response at 3.1 m depth was apparently from rise of groundwater. Assuming that the soil moisture response at 1.6 m depth at the eastern site is the wetting front from local precipitation, travel time of the wetting front was 59 mm/hr for the January 2–5, 2007, event and 44 mm/hr for a rainfall event on February 13–17, 2007 (Figure 5). A wetting front at the western site traveled to the WC-1s probe (1.5 m depth) at 154 mm/hr on January 2, 2007 (Figure 6), and 75 mm/hr on a similarly well-defined rainfall event on February 14–15, 2007 (Figure 5). Slower infiltration at the eastern site may be related to the 1.3 m of fill dirt there.

Piezometer Data

The pressures in each vertical array of grouted piezometers fall on a line consistent with estimated hydrostatic pressure, assuming that the piezometric head is close to the groundwater table (Figure 7). Head values in sand-packed piezometers were ~2.0 m lower than the estimated hydrostatic pressure and projected pressures observed from the grouted piezometer arrays (Figure 7). Data from the vertical arrays of grouted piezometers are only available for the first 4 months of 2007, whereas data from the sand-packed piezometers cover the entire 5 years.

Rainfall-induced vertical pressure transmission was tracked by vertical arrays of grouted piezometers through the deeper parts of the unsaturated zone at slightly higher rates than in shallower parts, but it was similar to corresponding rates of infiltration measured by the soil moisture probes (44–154 mm/hr). Intense rainfall on February 14, 2007, was preceded by nearly 3 weeks of negligible rain, creating the clearest response in the unsaturated zone for the 4 month observation period. In the western (LT-1a) borehole, the unsaturated piezometer responded after 132 hours after first increase in rainfall at 3.4 m depth (26 mm/hr), 199 hours at 9.1 m (46 mm/hr), and 263 hours at 15.2 m (58 mm/hr) (Figure 8). Vertical pressure transmission at the west site was 132 hours at 3.4 m (26 mm/hr), 199 hours at 9.1 m (46 mm/hr), and 263 hours at 15.2 m (58 mm/hr); at the middle site, it was 50 hours at 3.0 m (60 mm/hr). A linear regression through these data yields ~50 mm/hr ($R^2 = 0.84$) for the February 14–26, 2007, event; inclusion of the infiltration data from moisture probes also yields ~50 mm/hr ($R^2 = 0.90$).

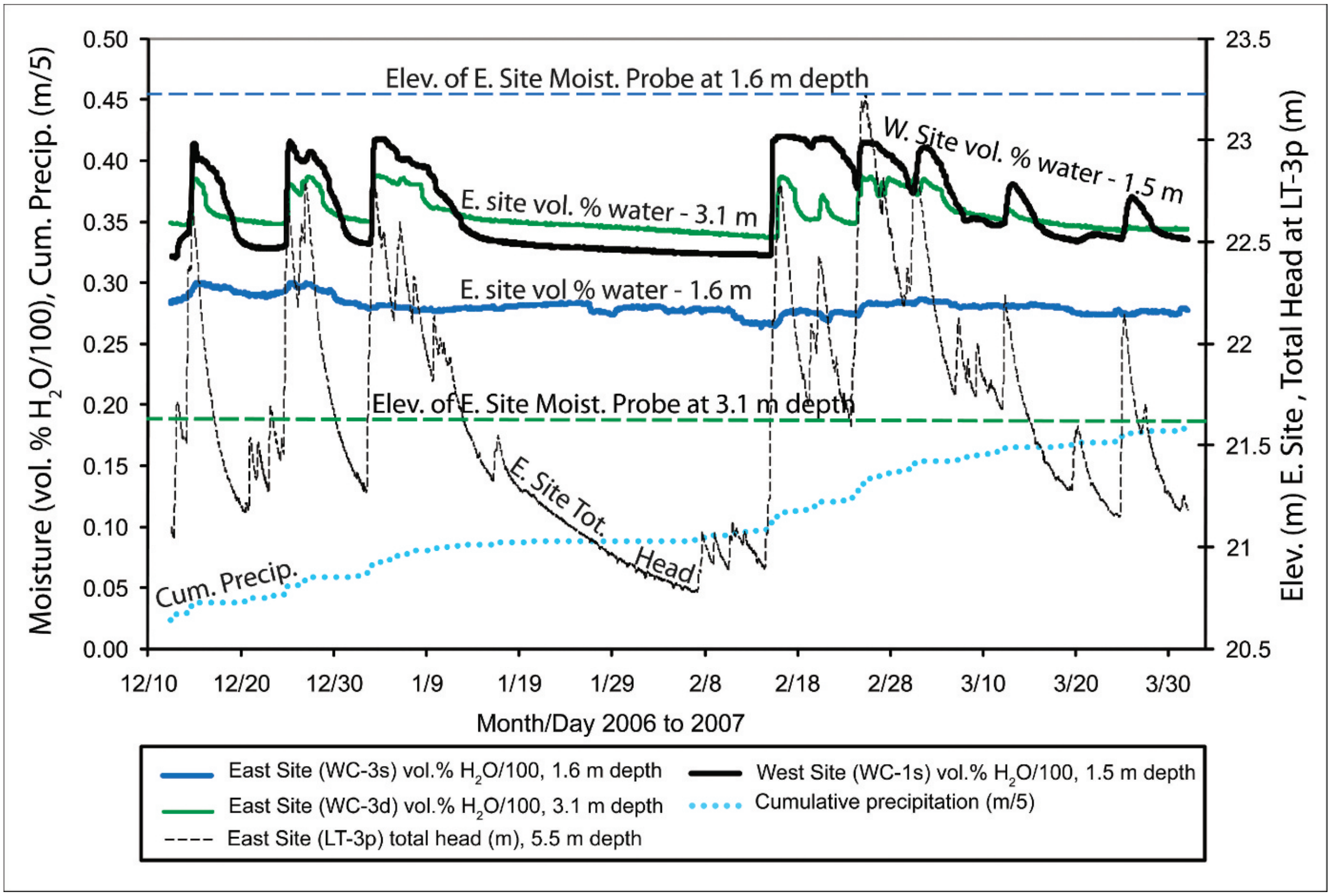

Figure 5. All 2006–2007 soil moisture observations at the western and eastern observation sites versus total head at the eastern site and cumulative precipitation. Elev. = elevation; precip. = precipitation; cum. = cumulative; W. = west; E. = east; moist. = moisture; vol. = volume.

Rainfall-induced waves of pore-pressure increase in the saturated zone progressed from the head to the toe of the slide much faster than can be explained by vertical infiltration or vertical pressure transmission through the unsaturated zone. For example, the piezometer at 21.3 m depth in the saturated zone nearest to the toe of the slide (LT-1 site) responded within 36 hours to the February 14, 2007, rainfall event, while the wetting front at this site had progressed just below 1.5 m without producing any pressure response in the piezometer at 3.4 m depth (Figure 8). Pore-water pressure perturbations from rainfall events generally arrived at the LT-3p site near the head of the slide within 15 minutes (Figure 9) to 90 minutes (Figure 6) of rainfall change, although arrivals were delayed as much as 2.75 hours (Priest et al., 2008). The initial pressure increases traveled laterally through the basal shear zone at speeds of ~1–6 m/hr between the east and middle sites and 1–5 m/hr between the middle and west sites (Figures 10 and 11). Arrival time of pore-pressure change varied little with depth and was far earlier than infiltration or vertical pressure transmission at all sites except at the head of the slide, where the piezometric surface and groundwater table are shallow (Figure 12). A sag pond in the head graben near the LT-3p piezometer (Figures 1 and 2) is further evidence of the shallow depth of the saturated zone there.

The piezometric surface slopes westward from the head to the toe of the slide and is steeper on the west side, intersecting the ground surface (or very nearly so) in the eastern head graben, and then falling to a depth of ~17 m at the western piezometers (Figure 13). The head above the basal shear zone is highest in the middle of the slide (Figure 13). Vertical hydraulic gradient is small, and flow direction inferred from the flow net of Figure 13 is roughly parallel to the slide plane and piezometric surface (Ellis et al., 2007a). The closer spacing of flow lines between the middle and western sites is consistent with higher hydraulic conductivity relative to the upper part of the slide (Figure 13).

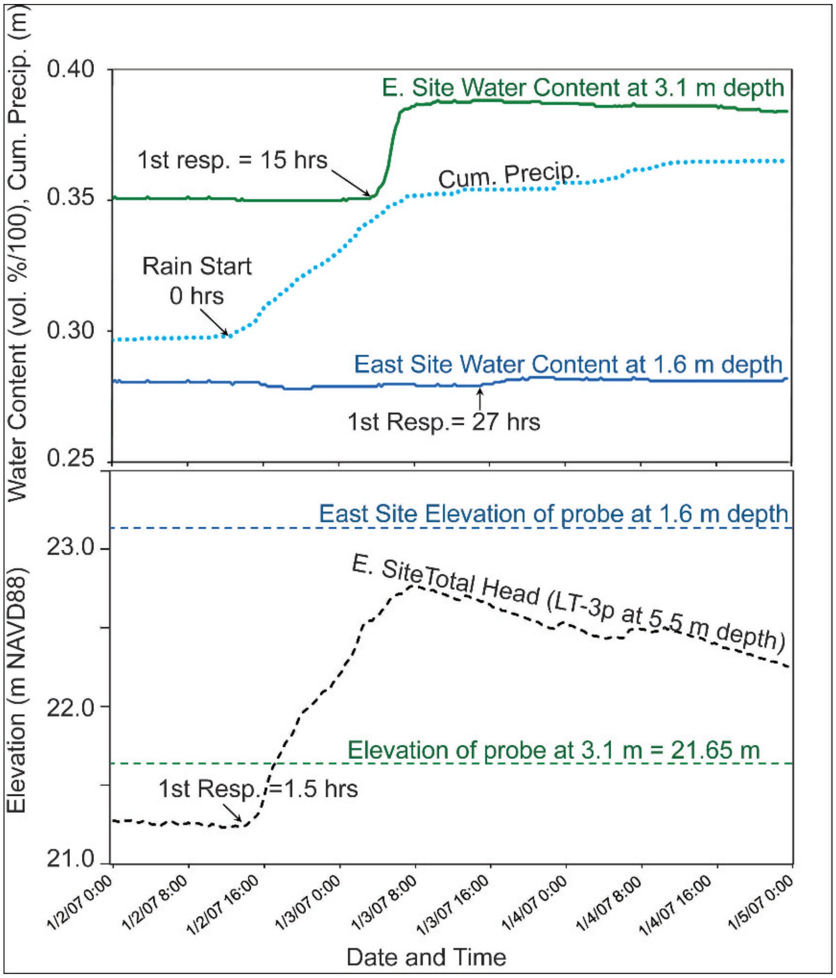

Figure 6. Soil moisture response (upper chart) compared to total head at the eastern site (LT-3p piezometer, lower chart) for a January 2, 2007, rainfall event. Deeper soil moisture probe responds before the shallow one, owing to rise of piezometric head. E. = east; Vol. = volume; Precip. = precipitation; Resp. = response.

Correlation of Movement to Pore Pressure

The threshold head above the slide plane for start and stop of movement had a maximum range of 3 m in the 2003–2004 hand-measured extensometer data, but only ~1 m once the automated system was installed in November of 2004 (Figure 14). The pore-pressure data illustrated in Figure 14 are for only the sand-packed LT-1p, LT-2p, and LT-3p piezometers, because they were installed for the entire observation period, thus eliminating previously discussed differences between pressures from grouted versus sand-packed instruments. For eight small movements recorded after precise, automated movement data became available, the threshold head above the slide plane for start and stop of movement at LT-1p, LT-2p, and LT-3p were ~6.2 ± 0.2 m, 8.7 ± 0.6 m, and 3.4 ± 0.5 m, respectively. Standard deviation from mean values increases from the west (LT-1) to the east site (LT-3), ~3 percent for LT-1p data, ~7 percent for LT-2p data, and ~15 percent for LT-3p data (Figure 14). There appears to be a general tendency for movement to start and stop at decreasing threshold head from 2003 to 2007, but the decrease is at most ~0.7–0.8 m of head, ~14–16 percent of normal summer-winter fluctuation, and is not significant relative to variance of the data (R^2 = 0.01–0.08; Figure 14).

The piezometric response and movement pattern for the largest movement and rainfall events that occurred in December 2002 and January–February 2003 were markedly different from all later events. Taking the February–March 2007 and December 2005–February 2006 events as examples of later events, the pressure response decreased in amplitude from the middle to the western site by factors of ~2–6 (Figures 15 and 16) relative to the January–February 2003 response (Figure 17). Movements in response to the pressure pulses in the 2005–2006 episodes began as near-equal movement at all sites followed by the

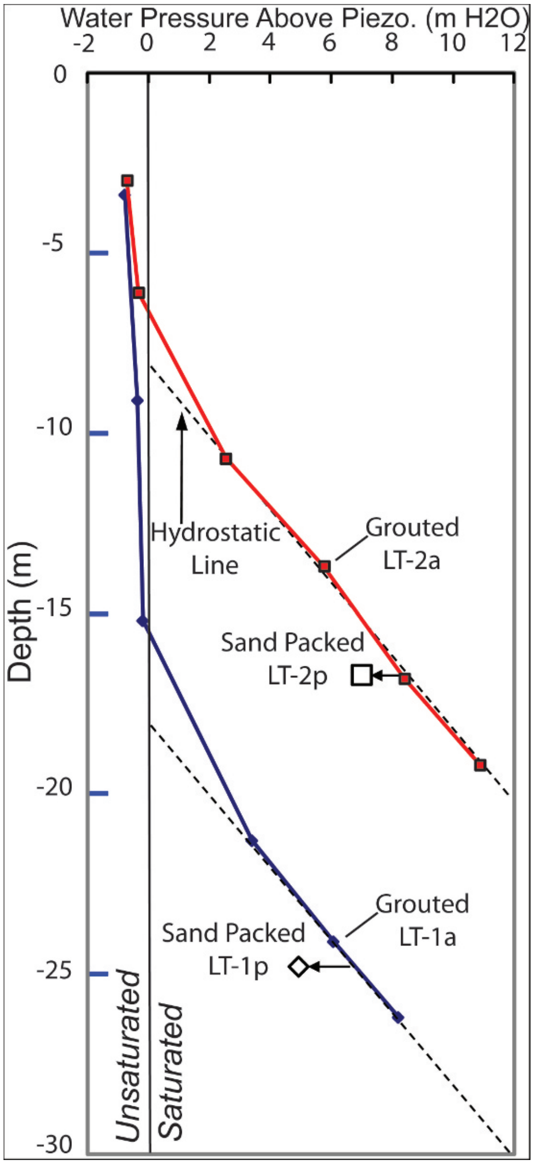

Figure 7. Variation of pressure with depth in vertical arrays of grouted piezometers (LT-1a and LT-2a) compared to two sand-packed piezometers in adjacent boreholes (LT-1p and LT-2p). Dashed lines depict ideal increase in water pressure with depth predicted by the weight of the water column in the saturated zone at each borehole (hydrostatic line). Piezo = piezometer.

middle site outpacing the other two as total movement exceeded ~2 cm (Figure 16). At the middle site, maximum velocity in 2005–2007 was 0.27 mm/hr, and maximum displacement was 9 cm. In contrast, the western site moved further than the other sites in December 2002 (Figure 17). In January–February 2003, the pulse of pressure at the western site nearly equaled that in the other sites (Figure 17). This pressure response was not repeated in the succeeding 4 years and accompanied the largest (21 cm) and fastest (6 mm/hr) movement. In the 2002–2003, 2005–2006, and 2007 examples, the east site appears to have reached a maximum rate of movement of ≤0.3 mm/hr and was essentially "left behind" by the middle site, where head above the slide plane is always highest (Figures 15–17). The eastern site also starts and stops movement at much more variable pore pressures than at the other two sites (Figures 15–17).

DISCUSSION

Monitoring at the Johnson Creek coastal landslide for 5 years allowed us to examine the factors controlling movement of large translational landslides in fractured sedimentary rock. The slide moves in response to intense rainfall that raises pore-water pressure throughout the slide over a period of 30–50 hours. The sequence of events that leads to movement starts with vertical infiltration and vertical pressure transmission through the unsaturated zone at ~50 mm/hr (~1.5–3.0 m depth in 30–50 hours). The piezometric surface slopes down the axis of the slide from near the ground surface at the head graben to a depth of about 20 m at the bluff crest above the landslide toe. Infiltration raises pore-water pressure in the graben within as little as 15 minutes, followed by lateral pressure transmission down the axis of the slide at speeds of 1–6 m/hr. Arrival time of this pressure "wave" or pulse occurs well before wetting fronts and associated vertical pressure pulses in the unsaturated zone reach the saturated zone in lower part of the slide (Figure 12). Exactly the opposite behavior occurs in slides with low hydraulic conductivity, such as the clay-rich Alani-Paty landslide in Hawaii, where movements are triggered by vertical rather than horizontal pulses of pressure through the saturated zone (Baum and Reid, 1995). For example, vertical pressure waves that trigger movement in the Alani-Paty landslide occur in response to bursts of intense rainfall, but only after the entire slide reaches near-complete saturation. The Johnson Creek Landslide is only fully saturated in the head graben, but the entire slide moves within hours of intense rainfall during the rainy season.

High hydraulic conductivity of the Johnson Creek Landslide is probably the cause of the relatively rapid lateral transmission of pore-water pressure. Vertical hydraulic gradient between the three monitoring sites is significant but small, indicative of flow roughly parallel to the west-dipping slide plane and groundwater table (Figure 13). The hydraulic gradient is about twice as high in the lower part of the slide as the upper part (Figure 13). These observations are consistent with a high effective saturated hydraulic conductivity throughout the slide mass, especially the lower part (Ellis et al., 2007a, 2007b). Since the rock matrix throughout most of the saturated zone is

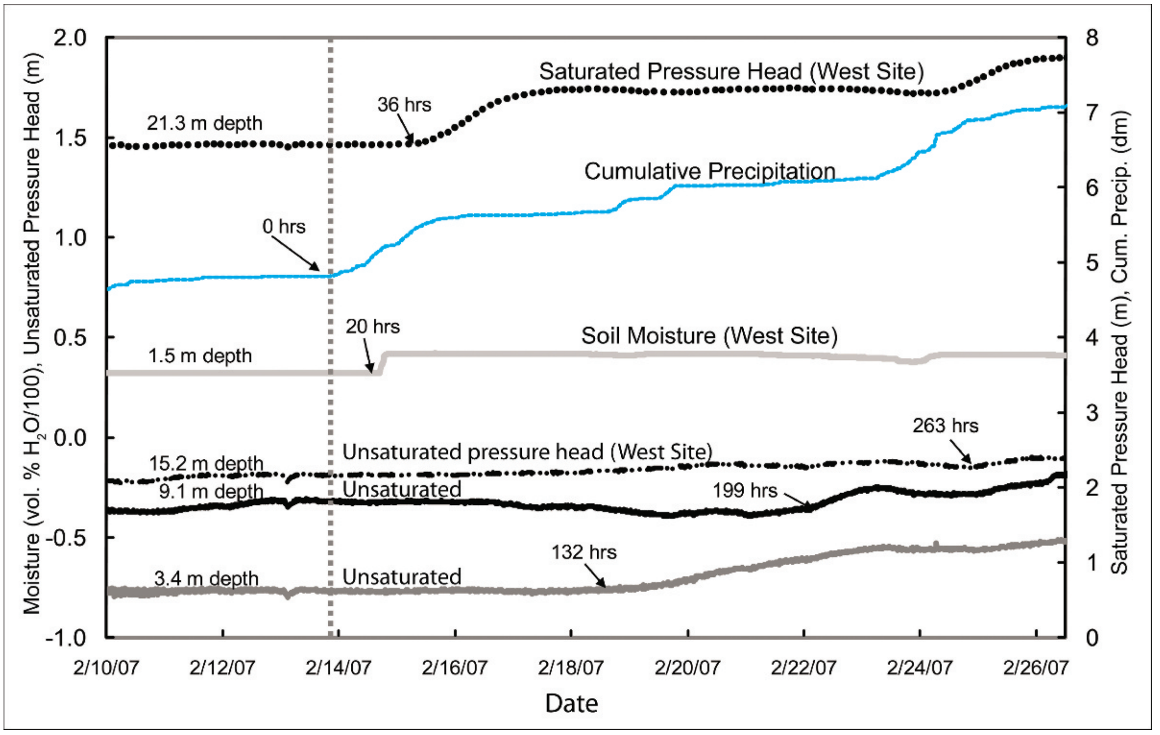

Figure 8. Response to rainfall at the west site for soil moisture probe WC-1S and grouted piezometers in borehole LT-1a. Depths are to piezometer or soil moisture probe tips. Hours are from the first increase in precipitation. Vol. = volume; Precip. = precipitation.

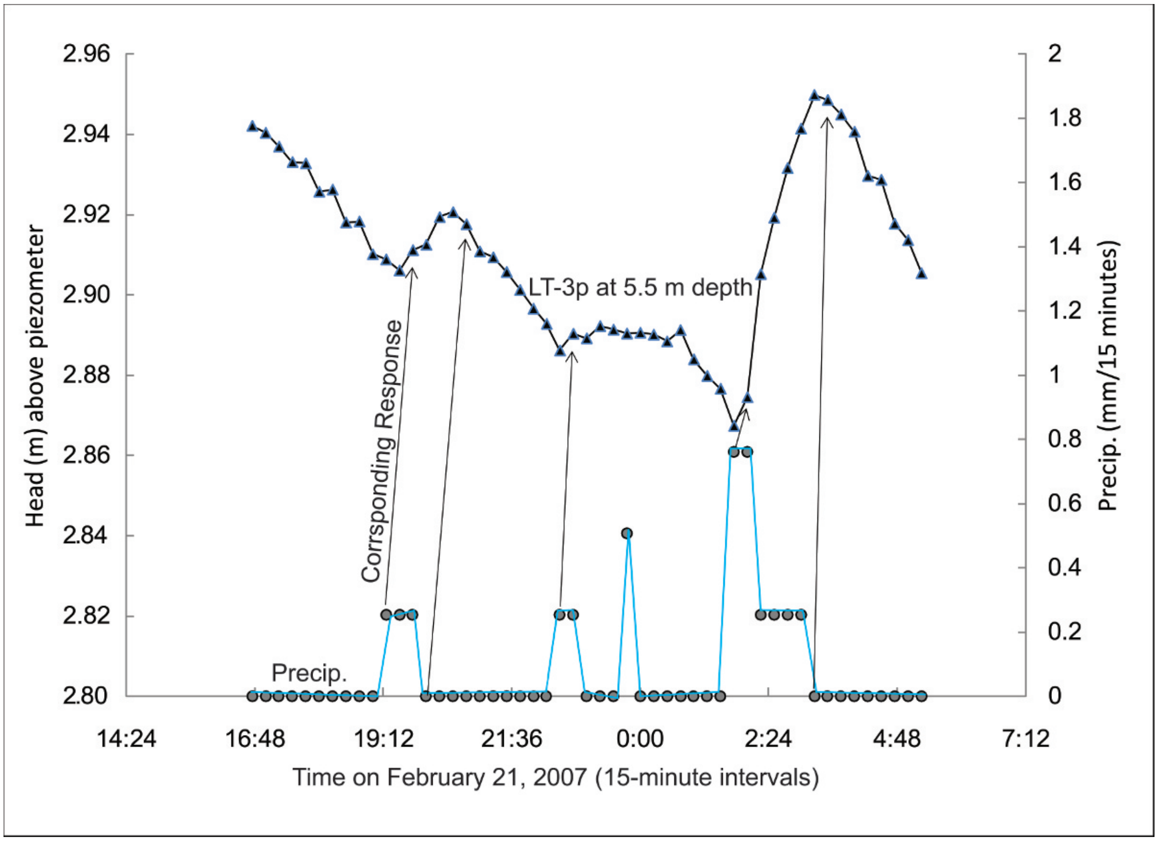

Figure 9. Pressure head response at the east site (LT-3p piezometer, black triangles) to rainfall (dark-gray dots) on February 21, 2007. Response at the LT-3p piezometer is utilized in the following figures as a proxy baseline for pressure responses to rainfall at the head of the landslide. Precip. = precipitation.

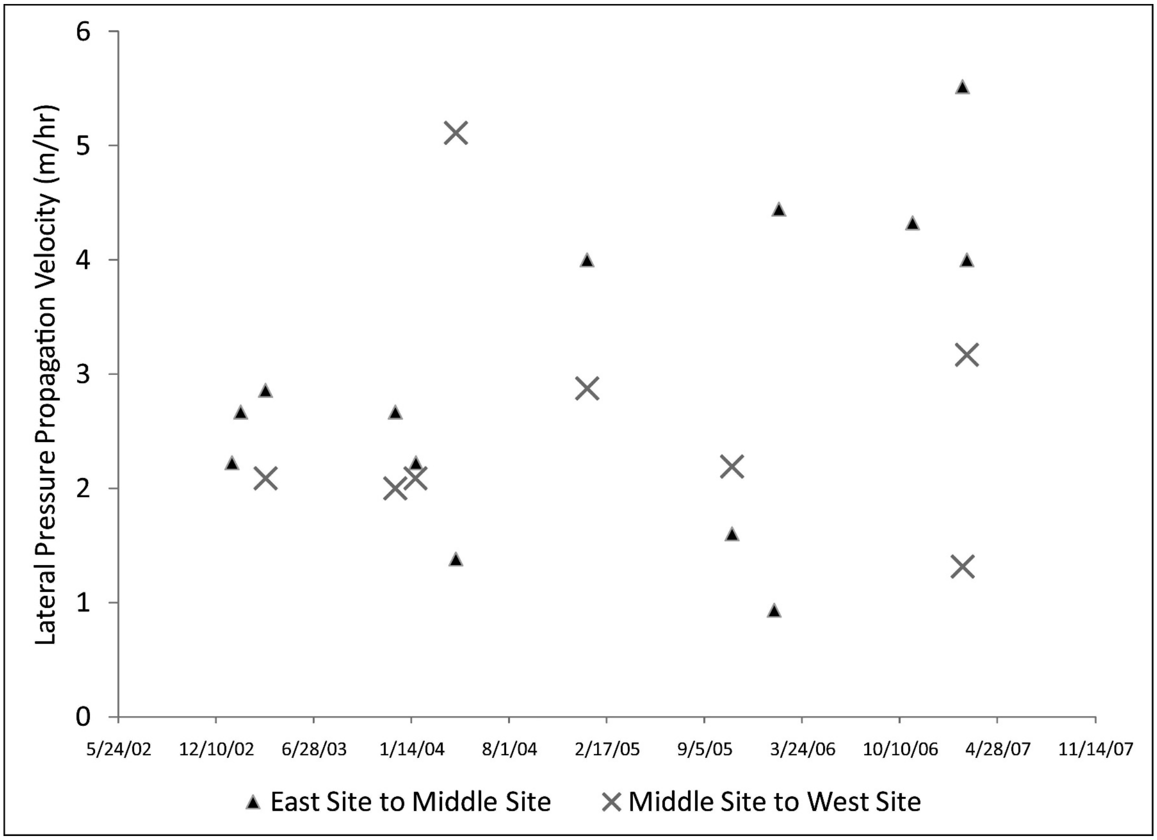

Figure 10. Velocities of lateral pore-pressure propagation through the basal shear zone at sand-packed piezometers LT-1p (west site), LT-2p (middle site), and LT-3p (east site at head of slide) at selected dates. On these dates, rainfall produced unambiguous pore-pressure responses in two or more of the piezometers.

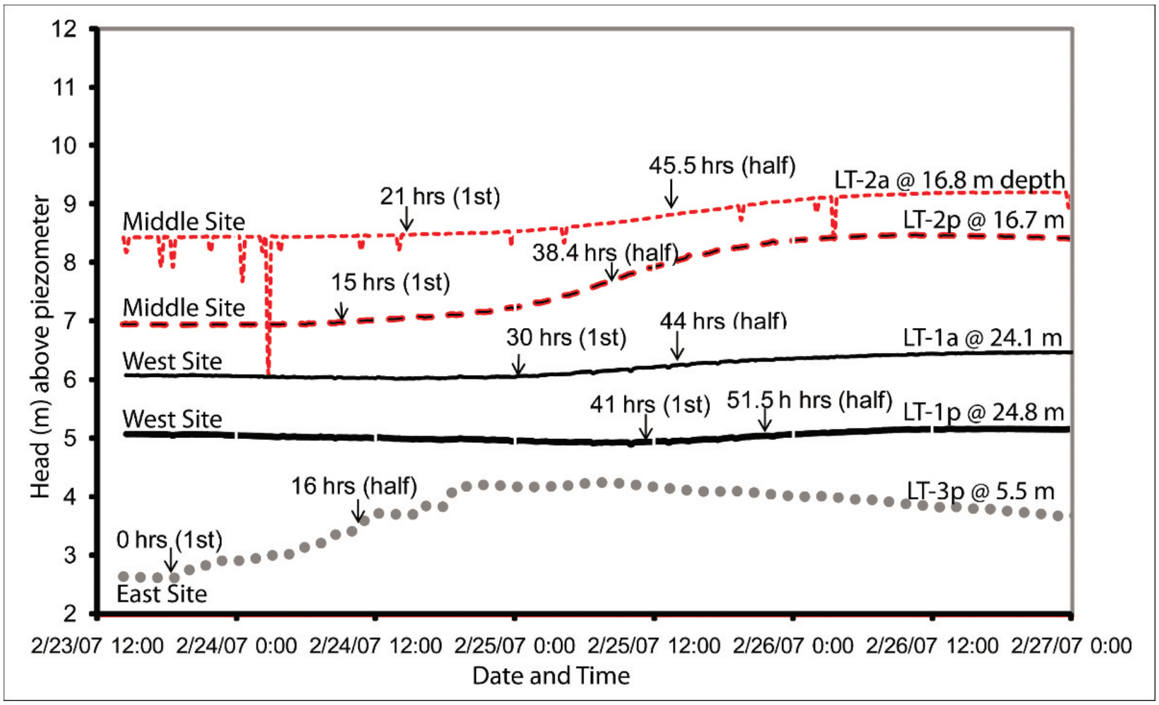

Figure 11. Timing of February 23–27, 2007, pressure head response down the axis of the slide relative to first response at the east (LT-3p) site on the west margin of the headwall graben. All data are from piezometers near the basal shear zone. LT-1p, LT-2p, and LT-3p are sand packed; LT-1a and LT-2a are grouted. 1st = first response; half = pressure reached half of the maximum perturbation; @ = at depth of.

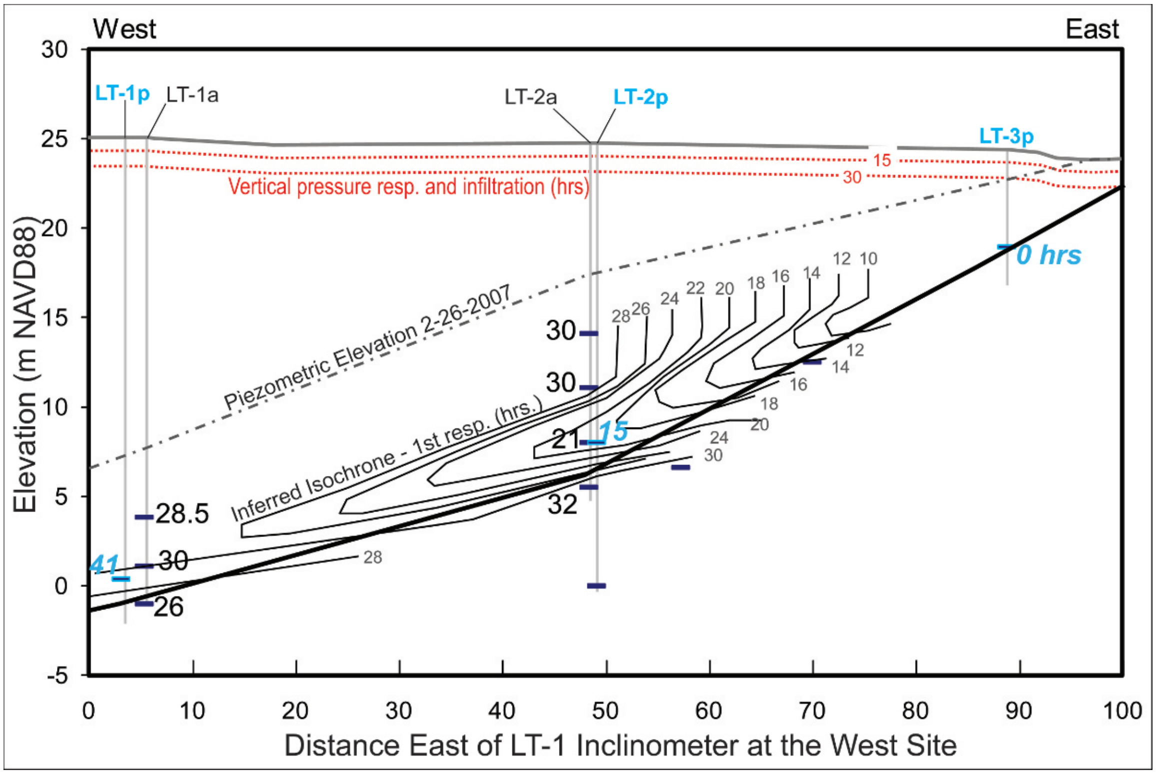

Figure 12. Pore-pressure response to a February 23–26, 2007, rainfall event. Isochrones are in 2 hour intervals interpolated from first response at grouted piezometers relative to first response at the LT-3p sand-packed piezometer. Piezometer depths are marked by horizontal bars with hours that response occurred for grouted piezometers (black) and sand-packed piezometers (blue, italic). Red dotted lines are isochrones for downward infiltration of groundwater and vertical pressure transmission through the unsaturated zone (~50 mm/hr). Vertical exaggeration is 1.6.

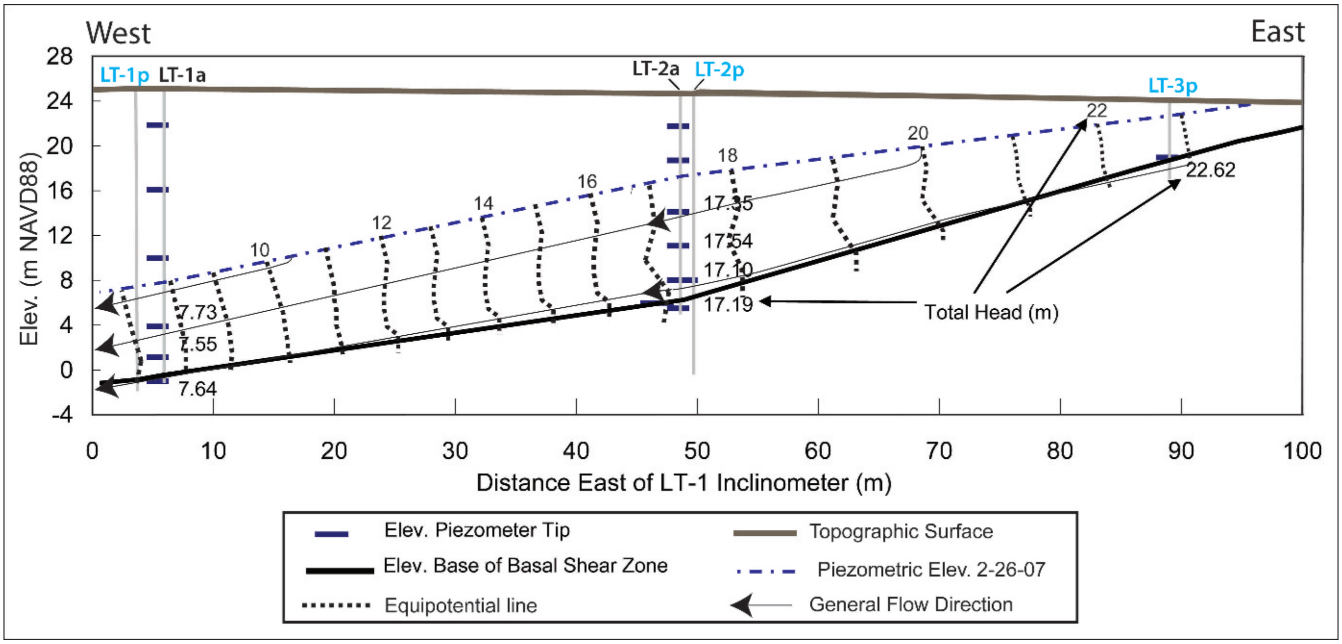

Figure 13. Groundwater flow net for February 26, 2007, a time of relatively high pore-water pressure. Numbers to two decimal places are measured total head at piezometers in boreholes LT-1a, LT-2a, and LT-3p. Total head differs little with depth in grouted piezometers in boreholes LT-1a and LT-2a, indicative of near-horizontal flow. Elev. = elevation relative to NAVD88; piezo = piezometer.

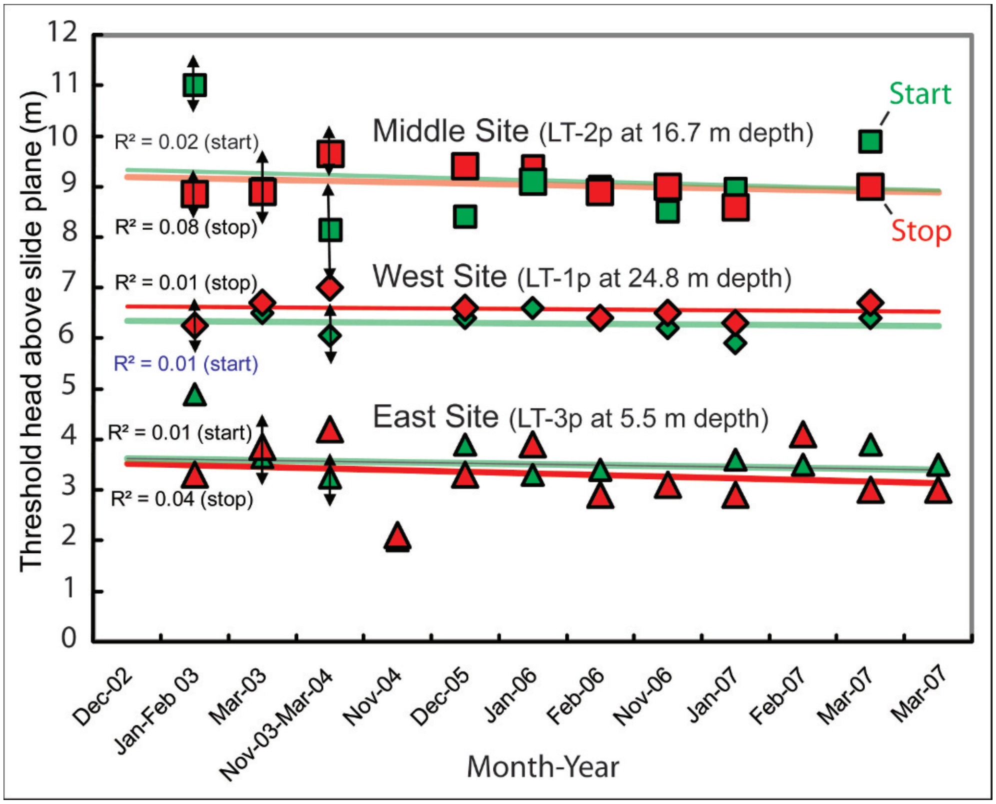

Figure 14. Variance of threshold head above the slide plane for start and stop of movement for all movement events. Arrows indicate uncertainty introduced because of large (1–4 day) sampling intervals and ±1 cm precision of extensometer data before automated recording of movement was available. Size of symbols without arrows is equal to or smaller than uncertainty in measurements. Lines are linear regressions through start (green) and stop (red) data with corresponding variances (R^2).

relatively impermeable siltstone and sandstone, high hydraulic conductivity is probably caused by the fractures observed in cores and outcrops. The basal shear zone is heavily brecciated, which should enhance hydraulic conductivity, particularly horizontal conductivity (K_h), relative to the rest of the slide mass. An apparent fault or internal slide structure that causes 2 m of down-to-the-east displacement of strata between boreholes LT-1 (western site) and LT-2 (middle site) (Figure 2B) probably also affects the observed head distribution (Landslide Technology, 2004; Ellis et al., 2007a).

The Johnson Creek Landslide has a brecciated basal shear zone with probable high K_h in close connection to a shallow groundwater table at the head of the slide, leading to extremely efficient transmission of lateral pore-water pressure. Lowering the groundwater table at the head of this slide through dewatering schemes should be an effective means of stopping or slowing slide movement.

Grouted vibrating-wire piezometers may be more accurate than sand-packed vibrating-wire piezometers for tracking the vertical and horizontal "waves" of pore pressure and for prediction of slide movement thresholds. The range of threshold pore pressures for slide movement for grouted piezometers in the basal shear zone is much narrower and better correlated to start and stop of movement than for sand-packed piezometers in adjacent boreholes (Figure 15). The grouted piezometers were also able to record the very small changes in suction pressure (−0.1 to −0.3 m) associated with rainfall-induced, vertical pore-pressure propagation in the unsaturated zone (Figure 8). Grouted piezometers installed at the same depth as adjacent sand-packed piezometers recorded saturated pore-pressure heads that were ~2 m higher during wet seasons (Figure 7). If one assumes that the groundwater table is approximated by the piezometric surface, as indicated by measurements from the vertical arrays of grouted piezometers, and that flow has an insignificant effect on pressure, then grouted piezometer pressures occur on the hydrostatic gradient, while sand-packed pressures were lower than the predicted hydrostatic pressure at the installed depth. However, flow through the saturated zone is not perfectly horizontal (Figure 13), so the small component of vertical flow may lower the head in the sand-packed piezometers. The ~3 m of sand around the

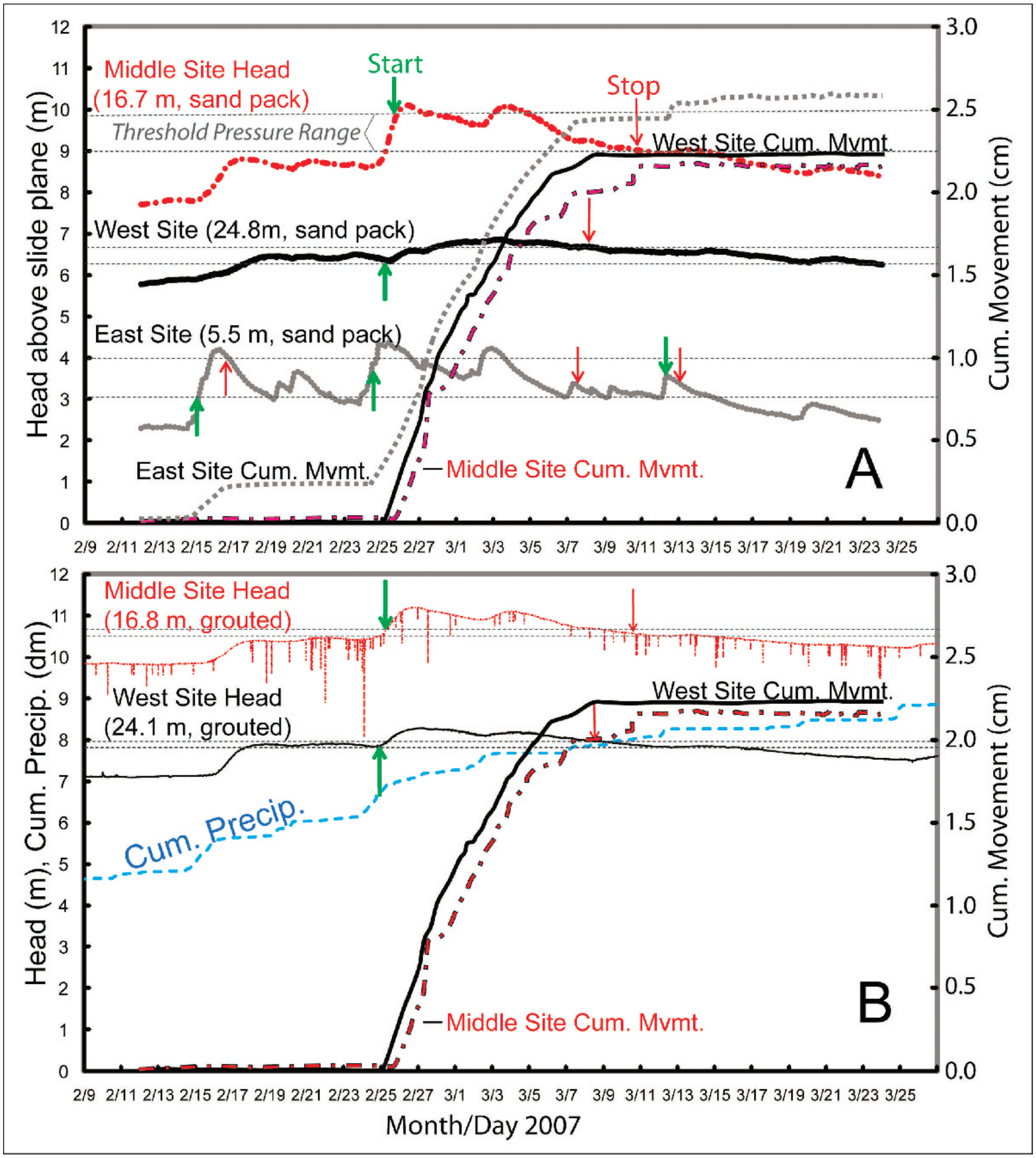

Figure 15. Correlation of movement to head above the basal shear zone for February–March 2007 slide movements in (A) sand-packed piezometers LT-1p (24.8 m depth, west site), LT-2p (16.7 m depth, middle site), and LT-3p (5.5 m depth, east site) relative to (B) nearby grouted piezometers LT-1a (24.1 m depth, west site) and LT-2a (16.8 m depth, middle site). Note the narrower range of threshold pressures for start and stop of movement in grouted relative to adjacent sand-packed piezometers. No grouted piezometers were installed at the east site, so no east site data are plotted in B. Cum. precip. = cumulative precipitation; cum. mvmt. = cumulative movement.

sand-packed piezometers and their location in the brecciated rock at the base of the slide probably enhance the opportunity for vertical flow.

Threshold pressures that triggered slide movement had a variance of ±0.2–0.5 m for the most precise data (Figure 14). This variance may be related to antecedent conditions such as the degree of saturation of the slide mass, changing lateral pressure distributions within the slide created by differential movement of neighboring blocks (Ellis et al., 2007a, 2007b), the relative importance of effective stresses at the monitoring locations, and the likely reduction in overall slide stability over the 5 years of observation as resisting toe material was removed by wave action; this latter factor is supported by the observed (though statistically insignificant) reduction in thresh-

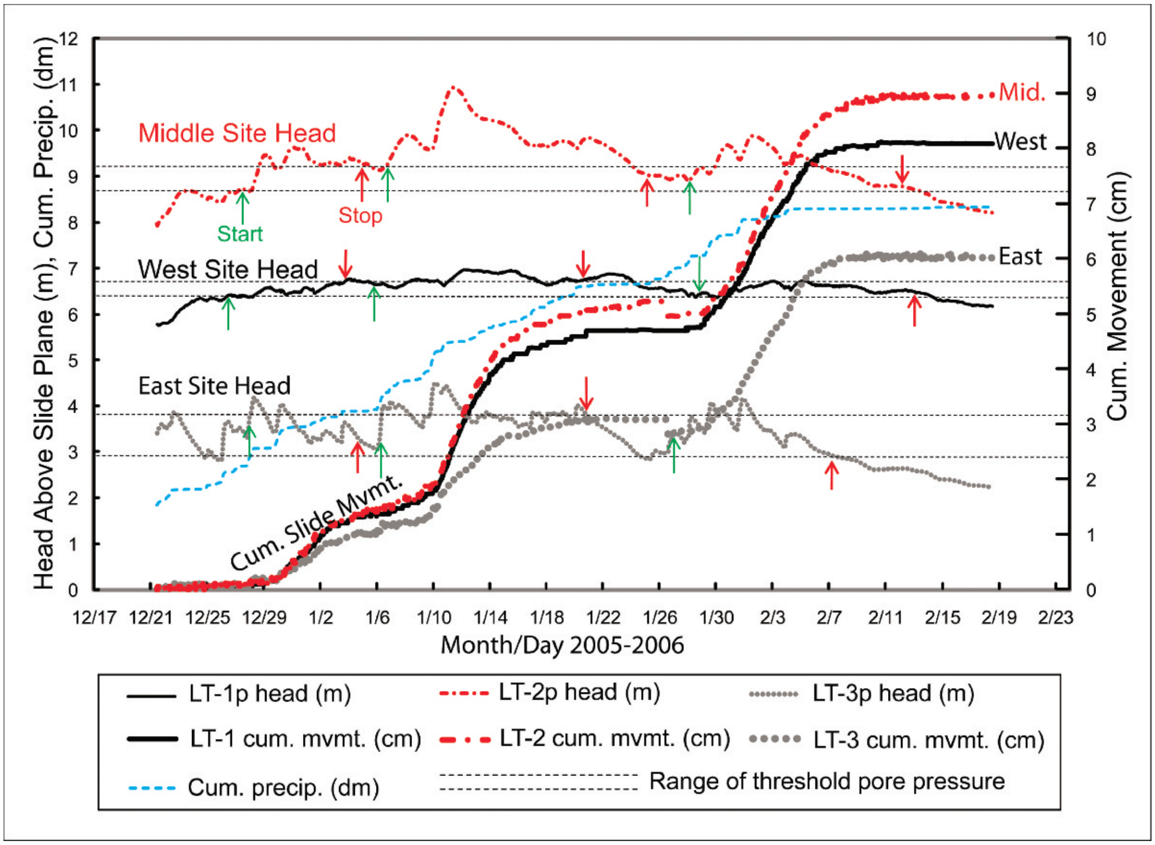

Figure 16. Correlation of movement to head above the basal shear zone in sand-packed piezometers for a December 2005–February 2006 slide movement. Piezometers are LT-1p (west site at 24.8 m depth), LT-2p (middle site at 16.7 m depth), and LT-3p (east site at 5.5 m depth); extensometers are LT-1 (west site), LT-2 (middle site), and LT-3 (east site). Data are for sand-packed piezometers in the basal shear zone. Cum. precip. = cumulative precipitation; cum. mvmt. = cumulative movement; mid. = middle extensometer site.

old heads with time (Figure 14). Part of the variance may be due to previously discussed potential error in the sand-packed piezometer data; however, measurements from the sand-packed piezometers cover a much longer time span (5 years) than those from the grouted piezometers (4 months), so time-varying processes may also have affected their variance.

Pore-water pressure change at the middle part of the slide appeared to be an important factor controlling movement. The middle monitoring site had head above the slide plane persistently higher than at sites to the east and west. Total movement there was a factor of 1.8 and 1.4 times that of the east and west sites, respectively (Table 3). The slide begins to move *en mass* when threshold pressures are reached, and the middle site (LT-2) outpaces the ones east and west when head at the middle site is ≥9.4–10.8 m above the slide plane. Pore-pressure thresholds for movement at the east site (LT-3 extensometer) near the headwall graben varied in complex ways not always well correlated to pore-pressure changes (e.g., Figures 15 and 16), consistent with passive response to movements at the middle part of the slide (LT-2 extensometer). For example, the February 15–16, 2007, movement of the site near the head graben (east site at LT-3) did not trigger movement down the axis of the slide (Figure 15A).

The lower part of the slide was also a critical control on stability. Pore-water pressure thresholds for movement in the lower part were much narrower and thus better correlated to movement than in the upper part of the slide (Figure 15). Only once in the 5 years of observation did the western site record as large of a pressure response to rainfall as the two sites higher on the slide (Figure 4A; compare Figure 17 to Figures 15 and 16); this unique response in February 2002 triggered movement an order of magnitude larger and faster than all others. The following conditions triggered the unique pressure response at the western site were: (1) rainfall of 0.84 m in the previous 60 days, (2) 2.1 mm/hr of rain in the previous 62 hours, and (3) 1 cm of extension between the western and middle sites created by greater movement in the western site in December 2002 (Figure 17 and Table 3). Extension should increase fracture permeability and thereby raise effective hydraulic conduc-

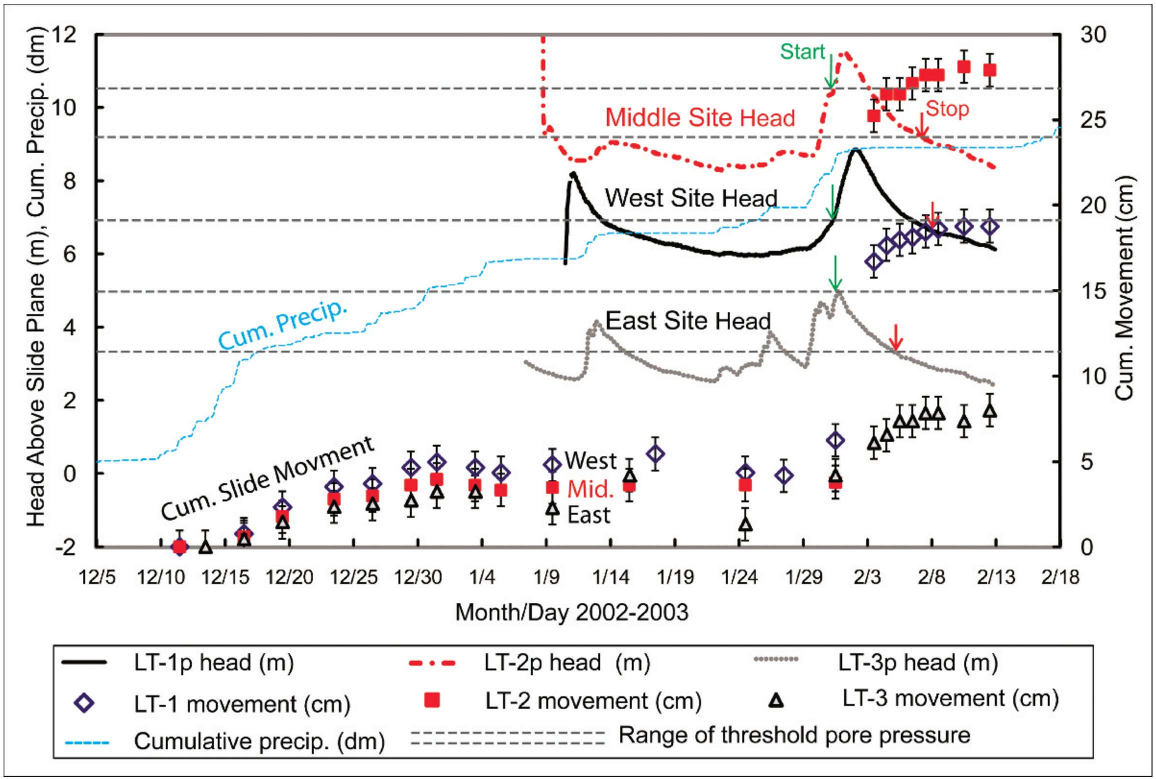

Figure 17. Correlation of movement to head above the basal shear zone for December 2002 to February 2003. The February event was the largest single movement during the 5 years of observation. Arrows mark head at start and stop of movement; thin dashed lines encompass the range of threshold pressure for start and stop. Piezometers are LT-1p (west site at 24.8 m depth), LT-2p (middle site at 16.7 m depth), and LT-3p (east site at 5.5 m depth); extensometers are LT-1 (west site), LT-2 (middle site), and LT-3 (east site). Only manually measured extensometer data were available during these observations, hence, the relatively large error bars and wide spacing in time of movement data. Cum. precip. = cumulative precipitation; mid. = middle extensometer site.

tivity. Such a rise in hydraulic conductivity in the saturated zone probably contributed to the large pore-pressure response at the western site. The resulting large movement in the middle site increased compression between the middle and western sites for the next 4 years. This compression probably decreased the effective hydraulic conductivity in the western part of the slide and contributed to the lack of large movements in the following 4 years. At some point in the future, the toe of the slide, perhaps in response to ongoing coastal erosion, may once again move more than the middle, opening up the fracture system and triggering faster, larger movements.

CONCLUSIONS

Five years of monitoring the Johnson Creek Landslide has demonstrated that rapid lateral transmission of rainfall-induced pore-pressure waves was a critical control of movement. Lateral pore-pressure transmission may be common in slides that share the following characteristics with the Johnson Creek Landslide: (1) high hydraulic conductivity in fractured bedrock, and (2) shallow groundwater table in some part of the slide, particularly at the head where the basal shear zone can be in close connection with a shallow groundwater table. Lowering the shallowest part of the groundwater table should be an effective means of slowing or stopping lateral pore-pressure transmission and resulting movement. This hypothesis and other remediation approaches were examined by Landslide Technology (2004) and Priest et al. (2008) through limit equilibrium modeling.

Other major findings are:

- Extension in the lower part of the slide mass appears to enhance pore-pressure response in the saturated zone, dramatically increasing speed and degree of slide movement; compression does the opposite. Destabilization by coastal erosion of the slide toe probably creates an alternating pattern of extension followed by compression in the lower part of the slide when the upper part "catches up."
- Vertical arrays of grouted vibrating-wire piezometers are an efficient means of tracking vertical and horizontal pressure transmission and may be more

accurate than sand-packed vibrating-wire piezometers. Grouted piezometers recorded a narrower range of threshold pore pressures for slide movement and higher pore pressure than adjacent sand-packed piezometers at the same depth.

ACKNOWLEDGMENTS

Oregon Department of Geology and Mineral Industries (DOGAMI) supervised the project with support by the Oregon Department of Transportation (ODOT) Miscellaneous Contract and Agreement, Project Name: "Detailed Geotechnical Analysis of Large Translational Landslides in Seaward-Dipping Sedimentary Rocks, State Planning and Research Project #356." Funding for the project was provided to ODOT by the Federal Highway Administration. In 2005–2006, essential labor and material support was provided by the U.S. Geological Survey (USGS) Landslide Hazards Program. Marshall Gannet, Jeff Coe, Rex Baum, and Dennis Staley of the USGS provided invaluable review and advice at various stages in the project. A technical advisory committee guided the project; members were Michael T. Long, Steve Narkiewicz, Bernie Kleutsch, and Matthew Mabey of ODOT, and Yumei Wang and William Burns of DOGAMI. Ian Madin of DOGAMI also provided helpful review.

Landslide Technology's team of geotechnical engineers and engineering geologists supervised initial drilling and produced a geotechnical report on the first year's work (Landslide Technology, 2004); their team included Charles M. Hammond, Andrew Vessely, Jonathan Harris, Erica Meyer, and Darren Beckstrand.

REFERENCES

Baum, R. L. and Reid, M. E., 1995, Geology, hydrology, and mechanics of a slow-moving, clay-rich landslide, Honolulu, Hawaii: *Geological Society of America Reviews in Engineering Geology*, Vol. 10, pp. 79–105.

Calabro, M. D.; Schmidt, D. A.; and Roering, J. J., 2010, An examination of seasonal deformation at the Portuguese Bend landslide, southern California, using radar interferometry: *Journal Geophysical Research*, Vol. 115, F02020, p. 10. doi:10.1029/2009JF001214.

Contreras, I. A.; Grosser, A. T.; and Ver Strate, R. H., 2008, The use of the fully-grouted method for piezometer installation, part 1: *Geotechnical Instrumentation News*, June 2008: pp. 30–37.

Corominas, J.; Moya, J.; Ledesma, A.; Lloret, A.; and Gili, J. A., 2005, Prediction of ground displacements and velocities from groundwater level changes at the Vallcebre landslide (Eastern Pyrenees, Spain): *Landslides*, Vol. 2, pp. 83–96.

Ellis, W. L.; Schulz, W. H.; Baum, R.; Priest, G. R., 2007a, Hydrogeologic investigations of the Johnson Creek Landslide; recent data, results and future plans. In Burns, W. J. and Wang, Y. (Compilers) "2007 Landslide Symposium Proceedings and field trip guide: New Tools and Techniques for developing regional hazard maps and future risk management practices": Oregon Department of Geology and Mineral Industries Open-File Report O-07-06, pp. 34–35.

Ellis, W. L.; Schulz, W. H.; and Priest, G. R., 2007b, Precipitation, pore pressure, and landslide movement—detailed observations at the Johnson Creek landslide, coastal Oregon. In Schaefer, V. R.; Schuster, R. L.; and Turner, A. K. (Editors), *Proceedings Landslides and Society: Integrated Science, Engineering, Management, and Mitigation, 1st North American Landslide Conference*: Special Publication 23, Association of Engineering Geologists, Denver, CO, pp. 921–934.

Fetter, C. W., 1994, *Applied Hydrogeology,* 3rd ed.: Macmillan College Publishing Company, Inc., New York, 691 p.

Iverson, R. M., 2000, Landslide triggering by rain infiltration: *Water Resources Research*, Vol. 36, No. 7, pp. 1897–1910.

Iverson, R. M. and Major, J. J., 1987, Rainfall, groundwater flow, and seasonal motion at Minor Creek landslide, northwestern California: Physical interpretation of empirical relations: *Geological Society of America Bulletin*, Vol. 99, pp. 579–594.

Landslide Technology, 2004, *Geotechnical Investigation of Johnson Creek Landslide, Lincoln County, Oregon*: Oregon Department of Geology and Mineral Industries Open-File Report O-04-05, 115 p.

McKenna, G. T., 1995, Grouted-in installation of piezometers in boreholes: *Canadian Geotechnical Journal*, Vol. 32, pp. 355–363.

Mikkelsen, P. E. and Green, G. E., 2003, Piezometers in fully grouted boreholes. In Myrvoll, F. (Ed.) *Proceedings of the Symposium on Field Measurements in Geomechanics, FMGM September 2003:* Oslo, Norway: AA. Balkema, Lisse, The Netherlands. FMGM = Field Measurements in Geomechanics, pp. 545–554.

Montgomery, D. R.; Dietrich, W. E.; and Heffner, J. T., 2002, Piezometric response in shallow bedrock at CB1: Implications for runoff generation and landsliding: *Water Resources Research*, Vol. 38, No. 12, 1274, doi:10.1029/2002WR 001429.

Priest, G. R. and Allan, J. C., 2004, *Evaluation of Coastal Erosion Hazard Zones along Dune and Bluff-Backed Shorelines in Lincoln County, Oregon: Cascade Head to Seal Rock*: Oregon Department of Geology and Mineral Industries Open-File Report O-04-09, 79 p., 7 appendices.

Priest, G. R.; Allan, J. C.; Niem, A. R.; Christie, S. R.; and Dickenson, S. E., 2006, *Interim Report: Johnson Creek Landslide Project, Lincoln County, Oregon*: Oregon Department of Geology and Mineral Industries Open-File Report O-06-02, 85 p., 10 appendices.

Priest, G. R.; Allan, J. C.; Niem, A. R.; Niem, W. A.; and Dickenson, S. E., 2008, *Final Report: Johnson Creek Landslide Research Project, Lincoln County, Oregon*: Oregon Department of Geology and Mineral Industries Special Paper 40, 76 p., 14 appendices, 1 data file.

Priest, G. R.; Allan, J. C.; Niem, A. R.; Niem, W. A.; and Dickenson, S. E., 2009, Movement triggers and remediation in a fracture-dominated translational slide at the Oregon coast: *Geological Society of America Abstracts with Programs*, Vol. 41, No. 7, p. 497.

Schulz, W. H., 2007, Hydrologic controls on translational bedrock landslides, coastal Oregon: *Geological Society of America Abstracts with Programs*, Vol. 39, No. 6, p. 362.

SCHULZ, W. H. AND ELLIS, W. L., 2007, *Preliminary Results of Subsurface Exploration and Monitoring at the Johnson Creek Landslide, Lincoln County, Oregon*: U.S. Geological Survey Open-File Report 2007-1127, 11 p., 1 appendix: Electronic document available at http://pubs.usgs.gov/of/2007/1127/

SCHULZ, W. H.; MCKENNA, J. P.; KIBLER, J. D.; AND BIAVATI, G., 2009a, Relations between hydrology and velocity of a continuously moving landslide—evidence of pore-pressure feedback regulating landslide motion?: *Landslides*, Vol. 6, pp. 181–190.

SCHULZ, W. H.; RICKARD, S. L.; AND HIGGINS, J. D., 2009b, Rapid response of deep bedrock landslides to rainfall, coastal Oregon: *Geological Society of America Abstracts with Programs*, Vol. 41, No. 7, p. 378.

SNAVELY, P. D., JR.; RAU, W. W.; AND WAGNER, H. C., 1964, Miocene stratigraphy of the Yaquina Bay area, Newport, Oregon: *The Ore Bin*, Vol. 26, No. 8, pp. 133–151.

TORRES, R.; DIETRICH, W. E.; MONTGOMERY, D. R.; ANDERSON, S. P.; AND LOAGUE, K., 1998, Unsaturated zone processes and the hydrologic response of a steep, unchanneled catchment: *Water Resources Research*, Vol. 34, pp. 1865–1879.

VAUGHAN, P. R., 1969, A note on sealing piezometers in boreholes: *Geotechnique*, Vol. 19, No. 3, pp. 405–413.